Geosynthetics, J. Kuwano & J. Koseki (eds)

Seismic stability of reinforced soil wall under different seismic waves using centrifuge shaking table tests

Izawa, J.
Department of Civil and Environmental Engineering, Tokyo Institute of Technology, Japan

Kuwano, J.
Geosphere Research Institute, Saitama University, Japan

Keywords: geogrid, centrifuge, shaking table test

ABSTRACT: This paper describes effects of input seismic wave properties on seismic stability of reinforced soil wall. For that purpose, the centrifuge shaking table test series was conducted with different waves. In the centrifuge test, behaviour and residual deformation of reinforced soil wall during earthquake were compared. As a result, it was found that acceleration response of the wall was almost the same along the wall height and deformation did not occur until the active acceleration exceeded the particular value. After the acceleration reached to that value, displacement of the model wall increased with shaking. Moreover, The relationships between shear stress and shear stiffness were determined by using the acceleration records. The shear modulus increased with shaking because the tensile stress was induced to the geogrid due to the deformation.

1 INTRODUCTION

Seismic behaviour of the reinforced soil wall depends on the properties of reinforcement and backfill soil. Authors investigated the effect of them by some centrifuge shaking and tilting table tests for past years (Izawa, et al. 1999, 2002, 2004). In addition to the componets of GRW, it is very important to consider the properties of seisimic wave for evaluating seismic stability of GRW. Therefore, some centrifuge shaking table test were conducted with some different waves and effects of input wave properties on seismic behaviour of the geogrid reinforced soil was studied.

2 OUTLINE OF THE CENTRIFUGE TEST

2.1 *Test procedure*

Tokyo Tech. Mark 3 Centrifuge and Horizontal Vertical 2D shaker (Takahashi et al. 2002) were used in this study. Figure 1 shows the configuration of the model geogrid reinforced soil wall, which was made with dense Toyoura-sand (Dr. = 80%, D_{50} = 0.19 mm, Uc = 1.56, ϕ = 42 deg.). Height of the wall was 150 mm and 5 pieces of geogrid with 90 mm length was arranged at the intervals of 30 mm. Model geogrid was made with polycarbonate plate with 1 mm thickness. Tensile strength and the friction angle with Toyoura sand was 506.8 kN/m and 38.6 degrees respectively. Each geogrid was attached to the divided panel made with aluminum plate. Schematic view of the model geogrid was indicated in Fig. 2.

Some displacement transducers and accelerometer were put in the model as shown in Fig. 1. Deformation

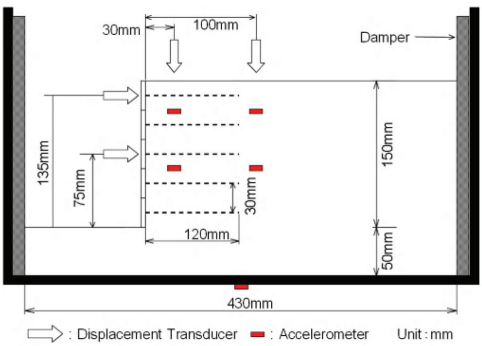

Figure 1. Configuration of the model setup.

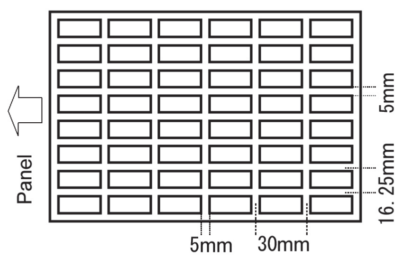

Figure 2. Schematic view of model geogrid.

Table 1. Seismic input waves.

Step	CASE 1 100 Hz Sin wave Number of wave	Acceleration (G)	CASE 2 100 Hz Sin wave Number of wave	Acceleration (G)
1	20	6.03	40	27.3
2	20	19.8	40	29.9
3	20	29.0	40	28.6
4	40	29.5	40	30.8
5	40	29.4	40	22.3
6	40	30.1	–	–

Step	CASE 3 1995 Hyogo-ken Nambu EQ Number of wave	Acceleration (G)	CASE 4 1993 Kushiro EQ Number of wave	Acceleration (G)
1	3.11	3.39	3.11	3.39
2	8.91	8.98	8.91	8.98
3	11.8	14.6	11.8	14.6
4	12.1	13.2	12.1	13.2
5	12.2	17.9*	12.2	17.9*
6	19.2*	17.6*	19.2*	17.6*

* frequency was 1/2 with prototype

of the model wall was observed by using CCDTV camera image processing system (Tyler. et al.). For this purpose, targets were put on the Perspex window of the container at 10 mm intervals.

2.2 *Input waves*

In this study, 4 types of input seismic waves were used. Properties and typical time histories of them are indicated in Table 1 and Fig. 3 respectively. Sinusoidal wave with a frequency of 100 Hz was applied to the wall in Case 1 and 2. Amplitudes of acceleration increased step by step in Case 1 as shown in Table 1. On the other hand, large acceleration, which was the same value with that of step 4 in Case 1, was applied to the model in Case 2 from the 1st step to the last step.

Irregular waves, which were observed at 1995 Hyogo-ken-Nambu earthquake and 1993 Kushiro earthquake, were used in Case 3 and 4 respectively. Amplitude and frequency of waves in Case 3 and 4 were different as shown in Table 1. Figure 4 shows the results of Fourier spectrum analysis of input accelerations in Case 3 and 4. Both of predominant periods of Case 3 and 4 were located near 60 Hz.

3 RESULTS AND DISCUSSIONS

3.1 *Natural frequency of the model*

Natural frequency of the model geogrid reinforced soil wall was determined by using Fourier analysis of acceleration records obtained from Case 3 and 4. Figure 5 shows the relationships between Fourier spectrum ratio (A11/A input) and frequency. Though

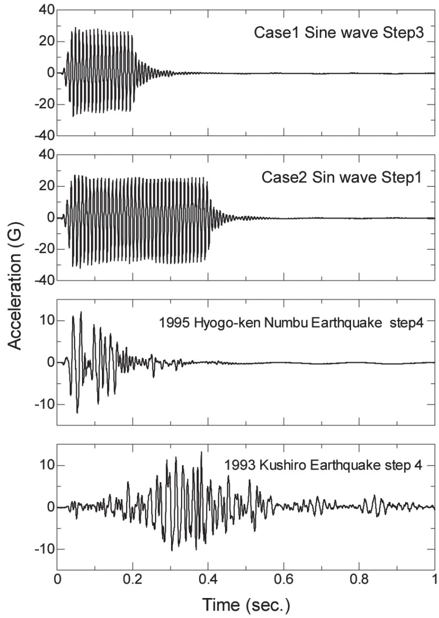

Figure 3. Examples of input wave.

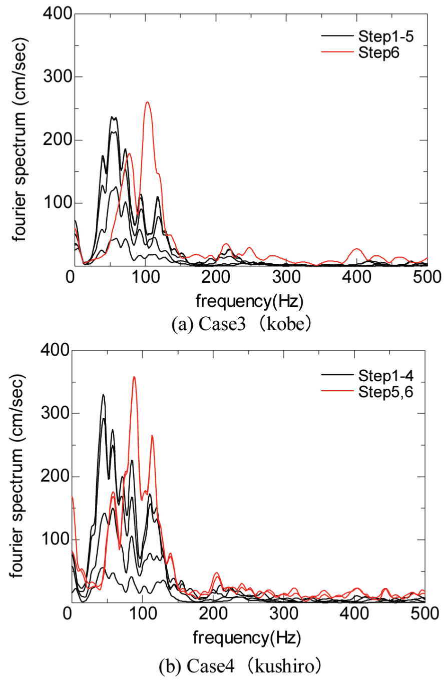

Figure 4. Fourier sepctra.

the stiffness of the model wall seems to change by deformation due to seismic motion, such behaviour was not observed in this study and peaks of the fourier spectrum ratios concentrated near 350 Hz in all cases.

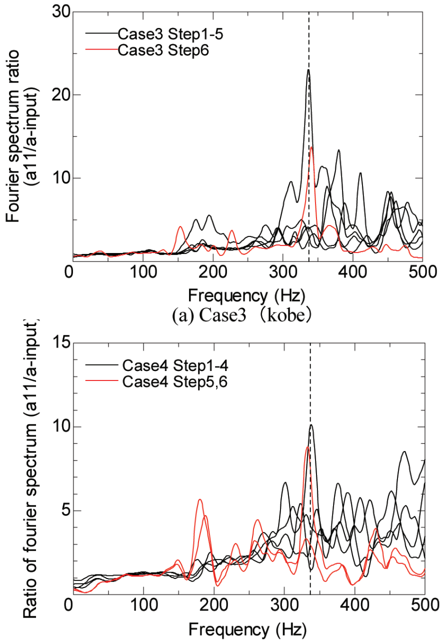

(a) Case3 (kobe)

(b) Case4 (Kushiro)

Figure 5. Fourier sepctrum ratio.

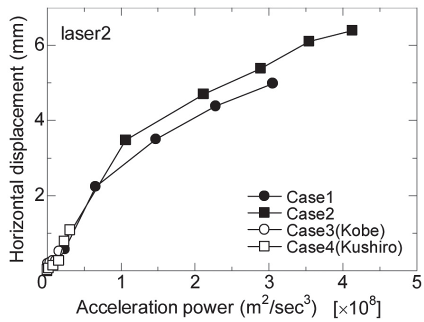

Figure 6. Horizontal displacement vs accelration power.

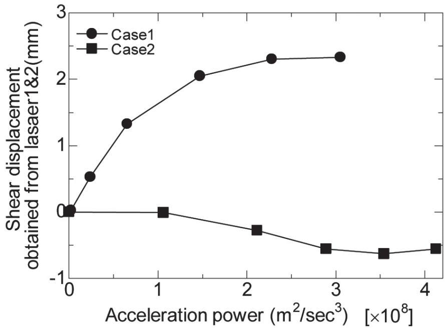

Figure 7. Shear displacement vs acceleration power.

That is, natural period of the model was located near 350 Hz. This value was much higher than predominant frequency of the waves used in this test series.

3.2 *Residual displacement*

Remarkable difference in residual displacement was not observed in Case 3 & 4 because displacement was restricted to very small. Figure 6 shows the relationships between horizontal displacement and acceleration power in Case 1 & 2. Acceleration power was used as a parameter to indicate the magnitude of earthquake motion and determined from a following equation.

$$T_E = \int_0^T a^2 dt \left(\begin{array}{l} a(\mathrm{m/sec}^2)\text{: acceleration} \\ \quad T(\mathrm{sec})\text{: shaking duration} \end{array} \right)$$

Progressive failure was not observed in all Cases and slopes of the curve, as shown in Fig. 6, decreased gradually with shaking. Large differences of residual displacement among all cases were not shown in Fig. 6. Shear displacement of Case 1 and 2, which were determined from the horizontal displacement obtained from laser 1 and laser 2, were indicated in Fig. 7. There is a clear difference between Case 1 and 2. Shear displacement increased with shaking in Case1. On the other hand, shear displacement was not observed in Case 2. The result indicated that displacement due to sliding was remarkable in Case 2.

3.3 *Deformation behaviour*

Figure 8 shows the time histories of horizontal displacement measured by laser 1, input acceleration and acceleration response (A11). At the beginning of earthquake, accelerations of input acceleration and A11 showed almost the same behaviour. When the input acceleration exceeded 10 G, deference of acceleration phase occurred and the horizontal displacement began to increase. Such behaviour was observed also in Case 4.

3.4 *Hardening of shear modulus of GRW*

Shear modulus was calculated by using acceleration records in order to investigate the increment of shear stiffness of GRW. Relationships between shear strain and shear stress were calculated by using acceleration records in Case 2. Assumed shear deformation and equation were shown in Fig. 9 (Koga, et al. (1990)). Here, the records were filtered by cutting out frequencies of less than 50 Hz and greater than 500 Hz and no residual strain was included in this result. Figure 10 shows the hysteresis and it was divided at the beginning, middle and end of the shaking. Skeleton curve as shown in Figure 10 roughly represent the secant shear stiffness. Figure 10 shows that the shear modulus increased with shaking. This indicated that shear stiffness increased during shaking. Tensile strain in geogrids generated due to the deformation of GRW

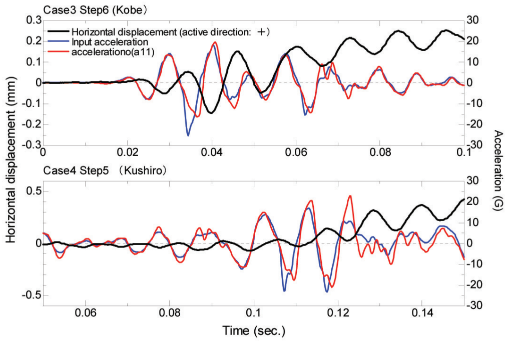

Figure 8. Time histories of horizontal displacement and acceleration.

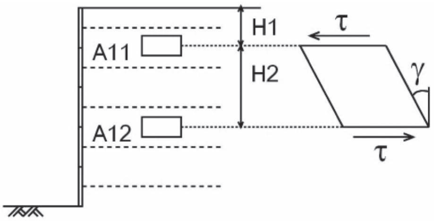

$$\tau = \rho H_1 a_1 + \rho \frac{H_2}{2} a_2 , \quad \gamma = \left(-\iint a_1 + \iint a_2 \right) / H_2$$ a: acceleration, ρ: density, H: Thickness of layer

Figure 9. Calculation of shear stress and strain from acceleration.

and tensile stress were applied to the geogrid. As a result, shear stiffness increased with increasing confining pressure applied to the backfill soil.

4 SUMMARY

1. Reinforced soil wall did not deform until the active acceleration was exceeded the particular value, which was about 10 G in this study. After the acceleration reached to the 10 G, displacement of the model wall increased with shaking. But strain hardening was observed and progressive failure did not occur.

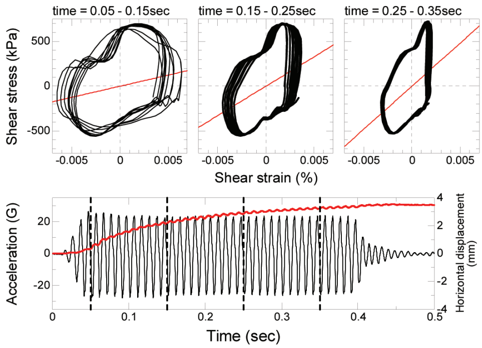

Figure 10. Relationships between shear stress and strain of reinforced zone.

2. The relationships between shear stress and shear stiffness were determined by using the acceleration records. As a result, it was found that the shear modulus increased with shaking because the tensile stress was induced to the geogrid due to the deformation.

REFERENCES

Izawa, J., Kuwano, J. and Takahashi, A. Behaviour of steep geogrid-reinforced embankments in centrifuge tilting tests, Proc. of ICPMG '02, pp. 993-998, 2002.

Izawa, J., Kuwano, J. and Takahashi, A. Centrifuge tilting and Shaking table tests on reinforced soil wall, Proc. of 7th Int. Conf. on Geosynthetics, pp. 229-232, 2002.

Izawa, J., Kuwano, J. and Ishihama, Y. Centrifuge Tilting and Shaking Table Tests on the RSW with Different Soils, Proc. of the 3rd Asian Regional Conference on Geosynthetics, pp. 803-810, 2004.

Koga, Y. and Matsuo, O. Shaking table tests of embankments resting on liquefiable sandy ground, Soils and Foundations, Vol. 30, No. 4, pp. 162-174, 1990.

Takahashi, A., Izawa, J. and Takemura, J. Dynamic behaviour of vertical geogrid-reinforced soil during earthquake, Slope Stability Engineering, Vo. 2, pp. 991-996, 1999.

Takemura, J., Takahashi, A. and Aoki, Y. Development of horizontal-vertical 2D shaker in a centrifuge, Proceedings of ICPMG '02, pp. 163-168, 2002.

Taylor, R.N., Robson, S., Grant. R.J. and Kuwano, J. Image acquisition using an on-board film camera, Centrifuge 98, pp. 67-72, 1998.